Mechanically Induced Solid-State Reaction for Synthesizing of Glassy Co75Ti25 Soft Magnet Alloy Powders with Wide Supercooled Liquid Region

doi: 10.1557/JMR.2002.0357

Mechanically induced solid-state reaction for synthesizing glassy $Co_{75}Ti_{25}$ soft magnet alloy powders with a wide supercooled liquid region

M. Sherif El-Eskandarany[a] and Wei Zhang
Inoue Superliquid Glass Project, ERATO, JST, Yagiyama-minami, 2-1-1, Sendai 982-0807, Japan
A. Inoue
Institute for Materials Research, Tohoku University, Katahira 2-1-1, Sendai 980-8577, Japan

(Received 29 January 2002; accepted 1 July 2002)

A single phase of glassy $Co_{75}Ti_{25}$ alloy powders was synthesized by high-energy ball milling the elemental powders at room temperature, using the mechanical alloying method. The final product of the glassy alloy, which is obtained after ball milling for 86 ks, exhibits soft magnetic properties with polarization and coercivity values of 0.67 T and 2.98 kA/m, respectively. This binary glassy alloy, in which its glass transition temperature (T_g) lies at a rather high temperature (833 K), transforms into face-centered-cubic Co_3Ti (ordered phase) at 889 K through a single sharp exothermic reaction with an enthalpy change of crystallization (ΔH_x) of −2.35 kJ/mol. The supercooled liquid region before crystallization ΔT_x of the synthesized glassy powders shows an extraordinary high value (56 K) for a metallic binary system. The reduced glass transition temperature [ratio between T_g and liquidus temperatures, T_l (T_g/T_l)] was 0.56. We also demonstrated postannealing experiments of the mechanically deformed Co/Ti multilayered composite powders. The results show that annealing of the powders at 710 K leads to the formation of a glassy phase (thermally enhanced glass formation reaction). Its heat formation was measured directly and found to be −0.56 kJ/mol. The similarity in the crystallization and magnetization behaviors between the two classes of as-annealed and as-mechanically alloyed glassy powders implies the formation of the same glassy phase.

I. INTRODUCTION

Over the past three decades, mechanically alloying (MA),[1] using the ball-milling and/or rod-milling[2] techniques has been employed for preparing several advanced engineering materials at room temperature.[3–5] Among these useful materials, metallic glassy alloys, with their unique short-range atomic order, have attracted many MA scientists[6–9] due to the desirable properties that make them pioneering materials for several industrial applications.[10–13] The worldwide interest in metallic glassy materials, which represent the ultimate state of solid metastability, has been sustained to a great degree by the clear benefits seen in the use of them in a number of application areas. Since the pioneering investigation of Koch *et al.*,[1] numerous numbers of amorphous alloys and metallic glasses were fabricated by the MA method.[14–23] Accordingly, the term MA is becoming increasingly common in both metal science and glass science.

In recent years, metallic glassy soft magnetic materials (see for example Refs. 24–27) have received much attention due to their unique properties and their promising applications. These materials offer the opportunity to decrease transformer core losses. In particular, a large elastic flexibility guarantees excellent insensitivity with respect to plastic deformations and a small electrical conductivity reduces the eddy-current losses. Co-based glassy/amorphous alloys, with their non-magnetorestrictive, possess excellent soft magnetic properties that favor them as core and sensor materials for inductive applications. Binary Co–Ti glassy alloys, which do not show any deep eutectic compositions in the equilibrium phase diagram,[28] have not received much attention because of the difficulties of preparation by the conventional melt-spinning method. The only report for the formation of an ordinary amorphous $Co_{78}Ti_{22}$ alloy by the way of rapid solidification from the molten metallic alloy was published by Inoue *et al.* in 1980.[29]

In this study, we have employed the ball-milling technique for fabrication of single glassy $Co_{75}Ti_{25}$ alloy powders, using the MA method. The effect of annealing on

[a]Address all correspondence to this author.
e-mail: msherif99@yahoo.com

the structure and stability of the multilayered Co/Ti composite powders, which are obtained during the early stage of milling, has been studied. For the purpose of this work, x-ray diffraction (XRD), scanning and transmission electron microscopy (SEM and TEM), vibrating-sample magnetometer (VSM), differential scanning calorimetry (DSC), and differential thermal analysis (DTA) have been employed to monitor the effect of MA time on the structural changes and the thermal stabilities of the fabricated glassy alloy powders.

II. EXPERIMENTAL

Pure elemental powders (99.9% or better) of Co (25 μm) and Ti (50 μm) were used as the starting reactant materials of MA. The powders were first balanced to give the nominal composition of $Co_{75}Ti_{25}$ (at.%), mixed, charged into tempered chrome steel vials (250 ml in volume), and then sealed together with 50 tempered chrome steel balls (10 mm in diameter) in an argon atmosphere glovebox. The ball-to-powder weight ratio was maintained as 14:1. The MA experiments were performed in a planetary ball mill (Fritsch P5) at a rotation speed of 2.1 s^{-1}. To avoid an increase in the vial temperature, the milling procedure was periodically interrupted every 1.8 ks and then halted for 3.6 ks under a continuous flow of air. The later process was necessary to eliminate the buildup of unprocessed powder deposits at dead or abandoned spots inside the vials. The ball milling was stopped after selected milling times (1.8, 3.6, 7.2, 11, 22, 30, 43, 54, 65, 70, and 86 ks), and a small amount (about 500 mg) of the MA samples was taken from the vials in the glovebox. The as-milled samples were characterized by means of XRD employing CuK_α radiation, high-resolution transmission electron microscopy (HRTEM) using a 300-kV field emission microscope, SEM using a 15-kV field emission electron microscope, DSC, and DTA at a constant heating rate of 0.67 K/s and under flow of a purified argon gas (99.999 wt%). The polarization (J_s) of the ball-milled powders was measured at room temperature, using a VSM with a maximum applied magnetic field of 670 kA/m. The coercive force was measured with a *B–H* loop tracer. Energy dispersive spectroscopy (EDS), using an electron beam of approximately 5 nm, has been used for analyzing the concentration of the alloying elements and the degree of Fe contamination in the milled powders. In addition, the oxygen content was determined by the helium carrier fusion thermal conductivity method. The iron and oxygen contamination contents in the final product (86 ks) of MA powders are 0.14 and 0.60 wt%, respectively. Annealing the multilayered composite MA powders was performed at the desired temperatures in well-sealed DSC Al cells under continuous flow (2.5 ml s^{-1}) of purified argon flow. As soon as the annealing procedure was achieved, the DSC was rapidly cooled and the samples were subsequently removed from the DSC heating chamber. The as-annealed samples were structurally analyzed by means of XRD, HRTEM/EDS, and VSM techniques. The SEM/EDS technique was employed to observe the metallographical and compositional changes of the as-annealed MA particles.

III. RESULTS

A. Structural changes with the MA time

The XRD patterns of as-milled $Co_{75}Ti_{25}$ powders are shown in Fig. 1 after selected MA times. In contrast to the powders of the early stage of MA (0 to 7.2 ks), which are a mixture of polycrystalline hexagonally close-packed (hcp)-Co and hcp-Ti [Figs. 1(a) and (b)], a broad diffuse and smooth halo appears after 32 ks of MA time [Fig. 1(c)], indicating the formation of an amorphous phase. This amorphous phase does not transform to any other metastable/stable phases even after longer MA time (86 ks), as displayed in Fig. 1(d).

The bright-field images (BFIs) of the powders at the early stage of milling are shown in Fig. 2. After a few kiloseconds of MA time (1.8 ks), the metallic Co and Ti

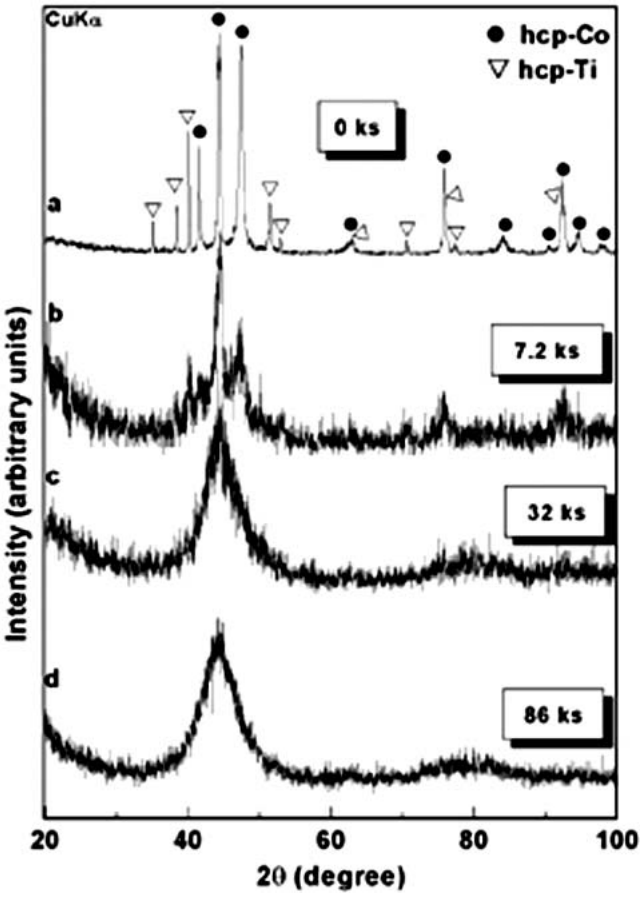

FIG. 1. XRD patterns of mechanically alloyed $Co_{75}Ti_{25}$ powders after (a) 0 ks, (b) 7.2 ks, (c) 32 ks, and (d) 86 ks of ball-milling time.

powders tend to agglomerate and form large-grain composite powders [Fig. 2(a)]. These agglomerated particles are continuously subjected to impact and shear forces upon increasing the MA time. The existence of numerous faults with grain boundary fringes and heavy dislocations in the boundary is the general feature for the sample, which was ball-milled for 7.2 ks [Fig. 2(b)].

The image of a HRTEM of the sample that was ball-milled for 86 ks is shown together with the corresponding selected area diffraction pattern in Fig. 3. The image shows maze pattern contrast [Fig. 3(a)] with a typical halo diffraction of an amorphous [Fig. 3(b)].

To assess the distribution of the alloying elements (Co and Ti) in the powders of the final product (86 ks), the local composition and the degree of homogeneity of the ball-milled sample have been examined by the HRTEM/EDS technique. Some selected examined regions for this sample are indexed in Fig. 3(a), and the corresponding EDS analyses are listed in the table that is placed in Fig. 3. Obviously, the compositions do not fluctuate drastically from region to region and the constituent elements of Co and Ti are almost uniformly distributed in the powders, being very closed to the starting nominal composition of $Co_{75}Ti_{25}$.

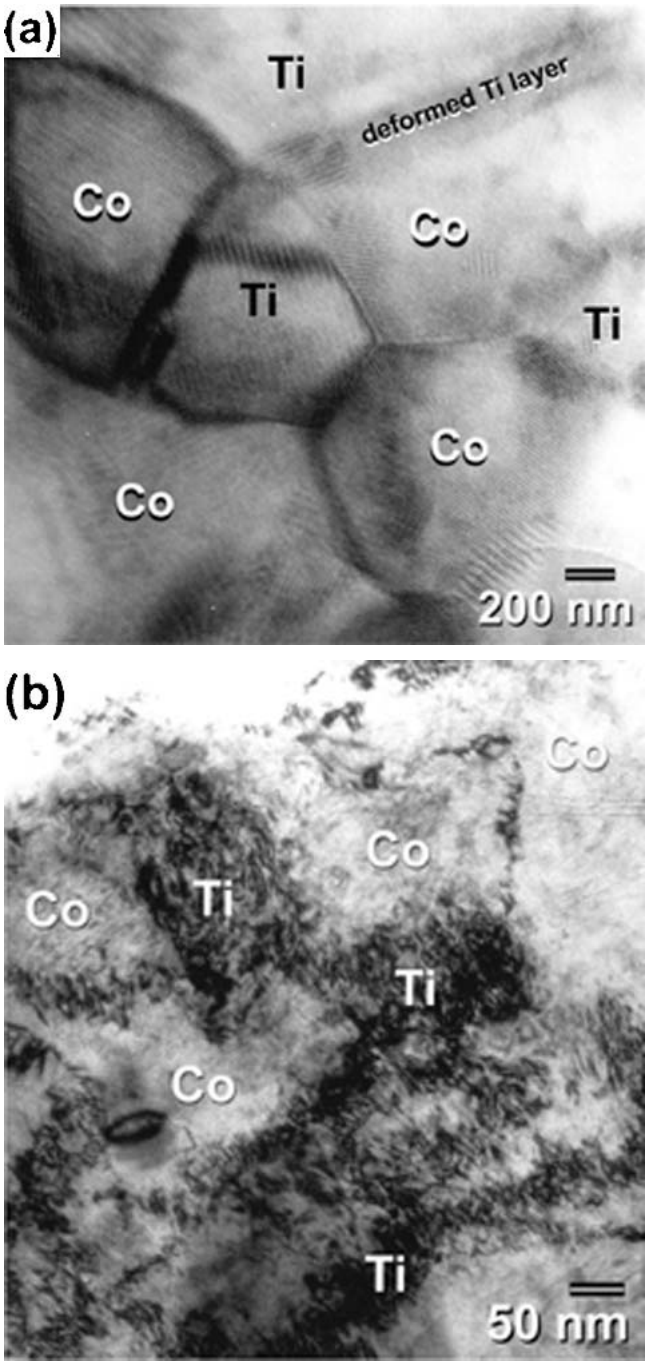

FIG. 2. BFI of mechanically alloyed $Co_{75}Ti_{25}$ powders after (a) 1.8 ks and (b) 7.2 ks of the ball-milling time.

B. Magnetic measurements

Since the magnetization is sensitive to the structure, the magnetic properties of mechanically alloyed $Co_{75}Ti_{25}$ powders are considered as powerful tools to monitor the phase transformations during the several stages of ball milling. The typical hysteresis *B–H* loops of some selected ball-milled $Co_{75}Ti_{25}$ alloy powders after different MA times are shown together in Fig. 4. Obviously, increasing the MA time leads to remarkable changes in the hysteresis *B–H* loops of the samples at the different stages of ball milling. In spite of the samples at the starting (0 ks) and early (7.2 ks) stages of ball-milling, which show rather high values of polarization (J_s) and coercive force (H_c), the sample at the intermediate (32 ks) stage possesses lower values. It is worth noting that the final product (86 ks), which is a single amorphous phase, exhibits a typical soft magnetic-type hysteresis loop (solid line in Fig. 4). The J_s and H_c of this end product are 0.64 T and 2.98 kA/m, respectively.

The J_s of the ball-milled $Co_{75}Ti_{25}$ powders is plotted as a function of the MA time in Fig. 5. The rapid decrease in the value of J_s during the early and intermediate stage of milling (0 to 43 ks) indicates a drastic decreasing of pure Co particles in the mixture of $Co_{75}Ti_{25}$ powders and the formation of an amorphous phase. After 54 ks of MA time, it decreases down to 0.67 T, indicating a continuous progress of the solid-state reaction between the diffusion couples of Co and Ti. Toward the end of the MA time (65 to 86 ks), J_s is almost saturated at a value of 0.64 T, suggesting the completion of the mechanically induced solid-state reaction and the formation of a single phase.

C. Thermal stability

Figure 6 displays the typical DSC scan of ball-milled $Co_{75}Ti_{25}$ powders at the early stage of MA (11 ks). The scan reveals three separated reactions that take place at

661 K (peak temperature of the first broad exothermic reaction), 765 K (onset temperature of the endothermic reaction), and 832 K (onset temperature of the second sharp exothermic reaction). We should emphasize that the first exothermic peak results from a temporary reaction and completely disappeared during the second heating run of a sample, which was previously annealed at 710 K. Contrary to this low-temperature reaction, the last two peaks remained during the second DSC scan. This low-temperature peak does not appear anymore in the DSC scans of the samples at the intermediate (22 to 43 ks) and final (65 to 86 ks) stages of MA, as shown in Fig. 7. Surprisingly, the endothermic reaction, which is clearly visible in the DSC scan (Fig. 6), disappears during the intermediate stage of the MA processing time [Figs. 7(a) and 7(b)]. Moreover, the second exothermic reaction, which takes place sharply in the DSC run of the 11 ks sample (Fig. 6), tends to be broadened with remarkable shift to the high-temperature side (857 K) upon MA for 22 ks [Fig. 7(a)]. The x-ray examination of the sample which was heated to 993 K [above the exothermic reaction in Fig. 7(a)] shows the existence of three phases; the first is an fcc-Co_3Ti (equilibrium phase), and the second and third phases belong to the unprocessed Co

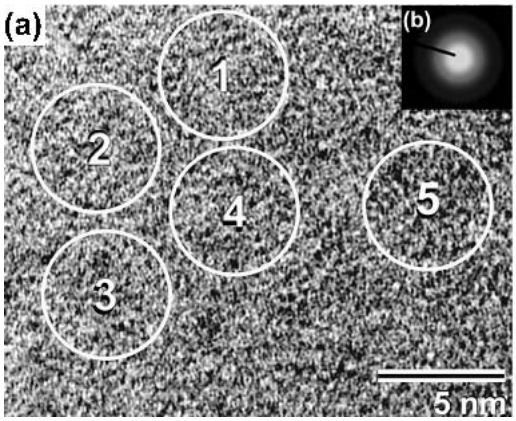

Region	Composition (at. %)	
	Co	Ti
1	75.7	24.3
2	76.3	23.7
3	75.2	24.8
4	74.7	25.3
5	75.8	24.2
av.	75.5	24.5

FIG. 3. (a) HRTEM and (b) the corresponding SADP of the final product (86 ks) of mechanically alloyed $Co_{75}Ti_{25}$ powders. The EDS analyses of some selected regions are listed in a table inset of the figure.

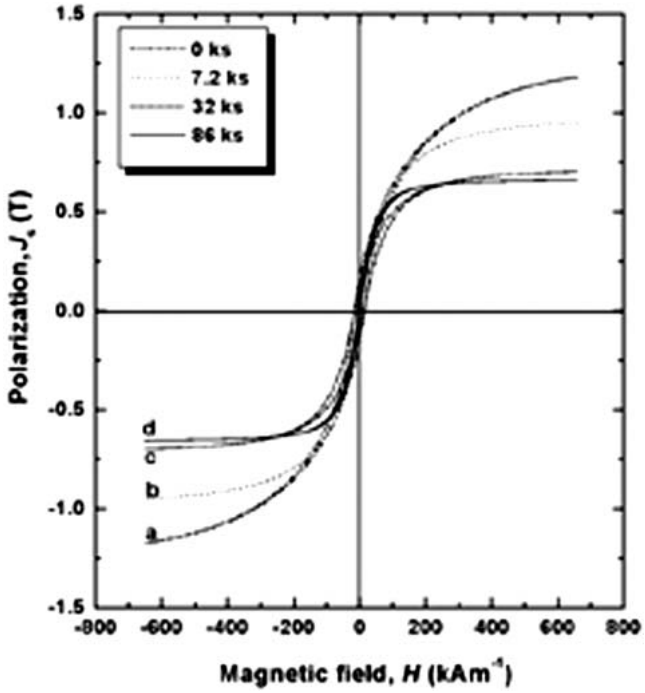

FIG. 4. Hysteresis B–H loops of as-mechanically alloyed $Co_{75}Ti_{25}$ powders after (a) 0 ks, (b) 7.2 ks, (c) 32 ks, and (d) 86 ks of the ball-milling time.

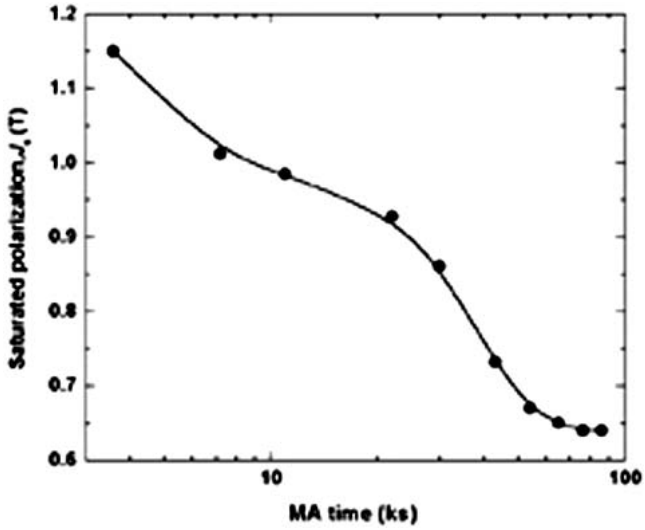

FIG. 5. Effect of the ball-milling time on the saturated polarization of mechanically alloyed $Co_{75}Ti_{25}$ powders.

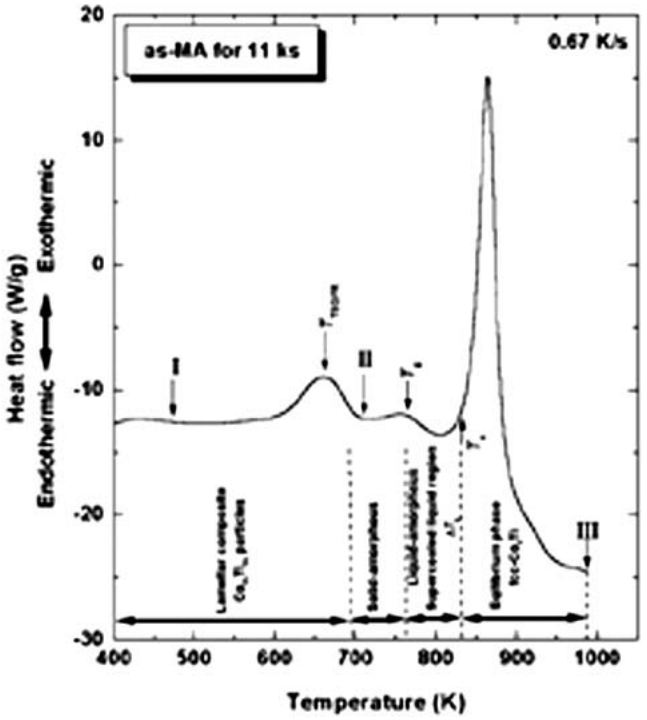

FIG. 6. Typical DSC curve of as-mechanically alloyed $Co_{75}Ti_{25}$ powders for 11 ks of the ball-milling time. Points I, II, and III refer to the samples that are taken for XRD, VSM, and TEM/EDS investigations (see Figs. 8–11). Whereas T_{TEGFR} is the peak temperature of the amorphization peak, T_g and T_x are the onset temperatures of glass transition and crystallization temperatures, respectively.

and Ti powders. Thus, we can conclude that the exothermic reaction, which appears in Fig. 7(a), belongs to the crystallization of the obtained amorphous $Co_{75}Ti_{25}$ phase. This crystallization reaction, however, becomes rather pronounced after 43 ks of MA time [Fig. 7(b)] and maintains its tendency for shifting to a higher crystallization temperature (T_x) side (876 K). The endothermic reaction that is corresponding to the glass transition temperature, T_g, appears at 833 K after 65 ks of MA time [Figs. 7(c)] and becomes more visible upon ball-milling for 86 ks, when the crystallization reaction becomes very sharp [Fig. 7(d)]. It is worth mentioning that the supercooled liquid region before crystallization, ΔT_x ($\Delta T_x = T_x - T_g$) of the end product (86 ks) exhibits an extraordinary wide value (57 K) for a binary metallic glassy alloy. The T_g was confirmed by heating the samples to a temperature just above T_g and then cooled to about 320 K. Then, second and third heating runs were performed to confirm the reproducibility of the T_g and to establish a base line. The T_g always appears at the same temperature (832.8 to 833.2 K) for all the three heating runs.

We shall return again to the scan in Fig. 6, with its puzzling low-temperature exothermic peak and thermal stability. To explore and interpret the roots of the fully separated exothermic reactions, three separated samples (denoted as I, II, and III), which had been originally ball-milled for 11 ks, were independently heated to the desired temperatures for several investigations. The SEM micrographs and their corresponding elemental (Co and Ti) dot mappings of polished and etched annealed powder are shown together in Fig. 8. The sample heated to 473 K (far below the first exothermic peak) reveals an intimate layered structure of the diffusion couples of Co and Ti, as presented in Fig. 8(a). Obviously, the elemental thin veins (varying from 1 to 7 μm in width) of Ti powders [Fig. 8(b)] are segregated in a good orientation to the Co matrix [Fig. 8(c)] with no indication of the formation of any single phase [Figs. 8(a)–8(c)]. The XRD pattern of this sample reveals sharp Bragg-peak reflections that correspond to elemental Co and Ti crystals, with no indication of the existence of a glassy phase [Fig. 9(a)]. In addition, its hysteresis B–H loop [Fig. 10(a)]shows rather high values of J_s and H_c, being very close to those values for the powders at the early stage of MA [see Figs. 4(a) and 4(b)], implying the absence of any glassy phase.

The lamellae that are shown in Fig. 8(a) disappeared [Fig. 8(d)] upon annealing the ball-milled powders at higher temperature (710 K) so that both elemental Co and Ti are uniformly distributed in the whole matrix [Figs. 8(e) and 8(f)]. This indicates the formation of a single phase. The XRD pattern of this sample that was

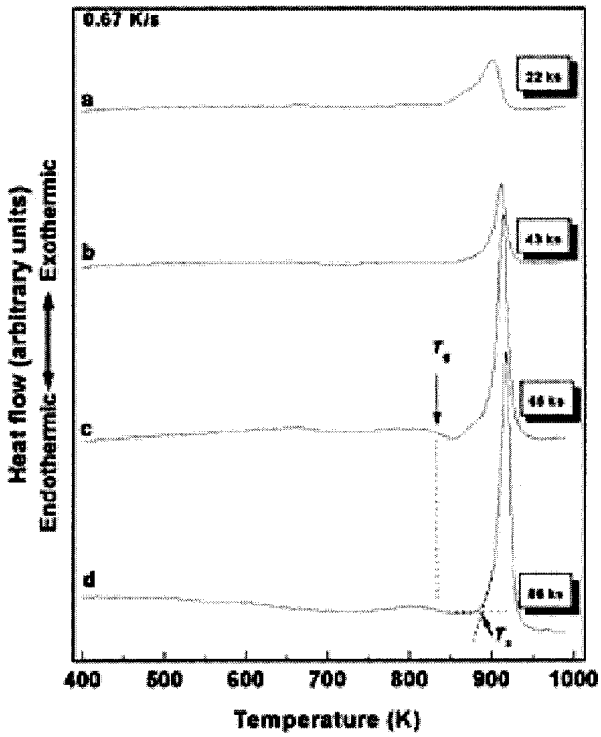

FIG. 7. DSC thermograms of mechanically alloyed $Co_{75}Ti_{25}$ powders after (a) 22 ks, (b) 43 ks, (c) 65 ks, and (d) 86 ks of the ball-milling time.

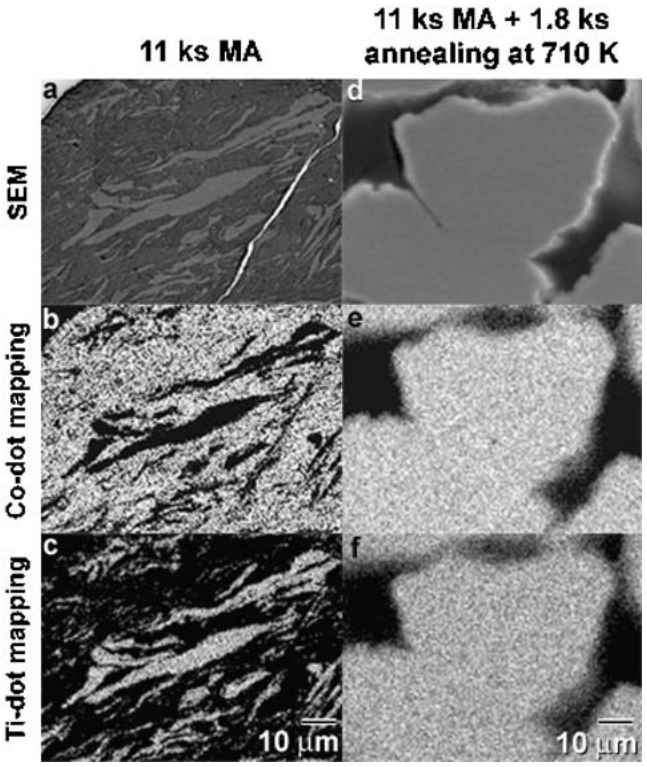

FIG. 8. (a) SEM micrograph and the corresponding elemental dot mapping of (b) Co and (c) Ti of mechanically alloyed $Co_{75}Ti_{25}$ powders after 11 ks of the ball-milling time. The SEM micrograph and its corresponding elemental dot mapping for the sample, which was annealed at 710 K after ball milling for 11 ks, are shown in (d)–(f).

taken after the completion of the first exothermic reaction (Fig. 6) reveals a typical halo-diffuse pattern of an amorphous phase [Fig. 9(b)]. In addition, it hysteresis *B–H* loop [Fig. 10(b)] shows lower values (in comparison with sample I) of J_s (0.68 T) and H_c (3.13 kA/m), being a little bit higher than those values of the glassy $Co_{75}Ti_{25}$ sample which is obtained after 86 ks of MA time [see Fig. 4(d)]. This may be attributed to the existence of unreacted elemental Co fine grains in the as-annealed sample. The local compositional analysis of this annealed sample has been examined by the HRTEM/EDS technique. Aside from the maze contrast of the HRTEM [Fig. 11(a)] and its correlated halo-diffuse selected-area diffraction pattern [Fig. 11(b)] of an amorphous phase, the compositions of some selected regions (see the table in Fig. 11) have close values with an average composition of $Co_{74.6}Ti_{25.4}$, being very closed to the starting nominal composition.

The XRD pattern of the sample that was heated to 993 K (sample III in Fig. 6) reveals an fcc structure with a lattice parameter (a_0) of 0.36175 nm, being in a good agreement with the reported value of the ordered phase of fcc-Co_3Ti.[30] Furthermore, the hysteresis *B–H* loop [Fig. 10(c)] does not imply any soft magnetic properties, with a low value of J_s (0.23 T).

In addition to the above analyses, the melting (T_m) and liquidus (T_l) temperatures of the as-annealed sample at 710 K have been examined, using the DTA technique. The typical DTA curve of the annealed sample is placed in Fig. 12(a) together with the DTA scan of the glassy powders that were obtained after 86 ks of MA time [Fig. 12(b)]. The curve a shows a single endothermic reaction which starts at 1425 K (T_m) and ends at 1480 K (T_l), in excellent agreement with the reported values of fcc-Co_3Ti.[28] These values are very close with those of the final product [1431 and 1476 K, respectively; Fig. 12(b)]; however, the T_g/T_l value of as-annealed sample (0.52) is rather lower than that one of the final product (0.56). Therefore, it can be concluded that when pure multilayered $Co_{75}Ti_{25}$ composite particles are subjected to isothermal annealing at 710 K for 1.8 ks, a solid-state diffusion reaction is taking place and a glassy phase is yielded. We shall call this process a thermally enhanced glass formation reaction (TEGFR).

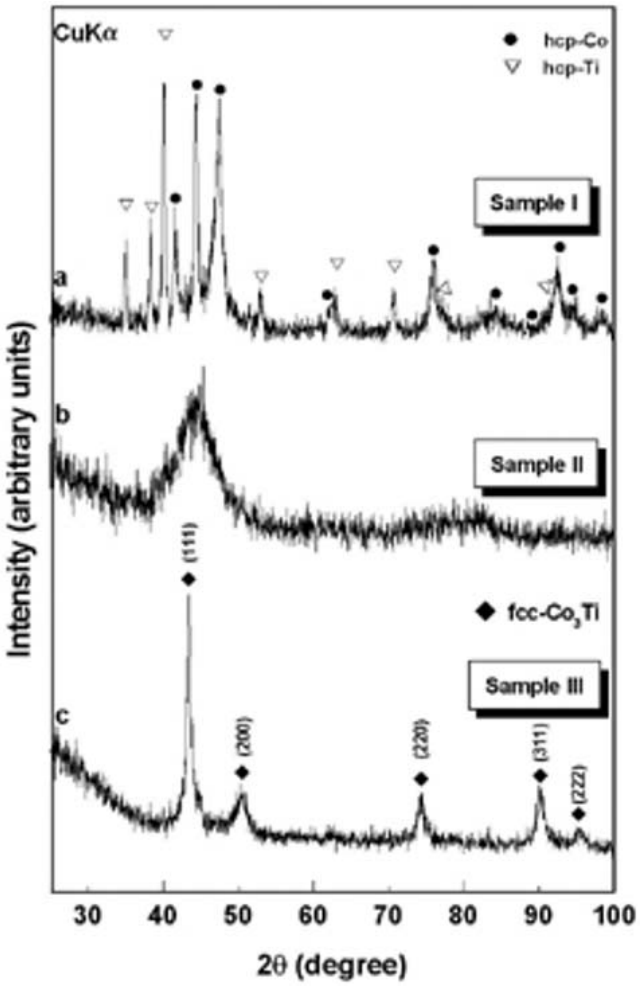

FIG. 9. XRD patterns of previously mechanically alloyed $Co_{75}Ti_{25}$ powders for 11 ks and then heated to (a) 473 K, (b) 710 K, and (c) 993 K (see Fig. 6).

The thermal stability of mechanically alloyed $Co_{75}Ti_{25}$ powders, indexed by the T_g, and crystallization temperature, T_x are presented together as a function of the MA time in Fig. 13. In the figure, the T_{TEGFR} (peak temperature of the low exothermic temperature reaction in Fig. 6), which takes place during the early stage of milling, is independent of the MA time and disappears after 11 ks of the MA time. At this early stage of milling, T_g appears at a temperature range of 760 to 766 K and surprisingly disappeared as soon as T_{TEGFR} disappears. The T_x of the glassy phase that obtained at the early stage of milling slightly changes with increasing MA time. It, however, changes dramatically during the intermediate stage, indicating continuous compositional changes of the mechanically alloyed powders. At the end of the final stage of milling (65 to 86 ks), T_x tends to get a saturated value of 889 K, implying the completion of the mechanically induced glass formation reaction (MIGFR) and the formation of a single homogeneous phase. Moreover, T_g, which disappeared during the intermediate and the midparts of the final stages of milling, appears during the end of this final stage (76 to 86 ks). ΔT_x of the glassy phase that was obtained at the final stage of milling has a rather large value of 56 K. This value is rather lower than that of the glassy phase, which is obtained by annealing the powders of the early stage of milling (63 K). This may be attributed to introducing oxygen and iron contaminations to the powders (0.14 and 0.60 wt%, respectively) upon longer ball milling (86 ks).

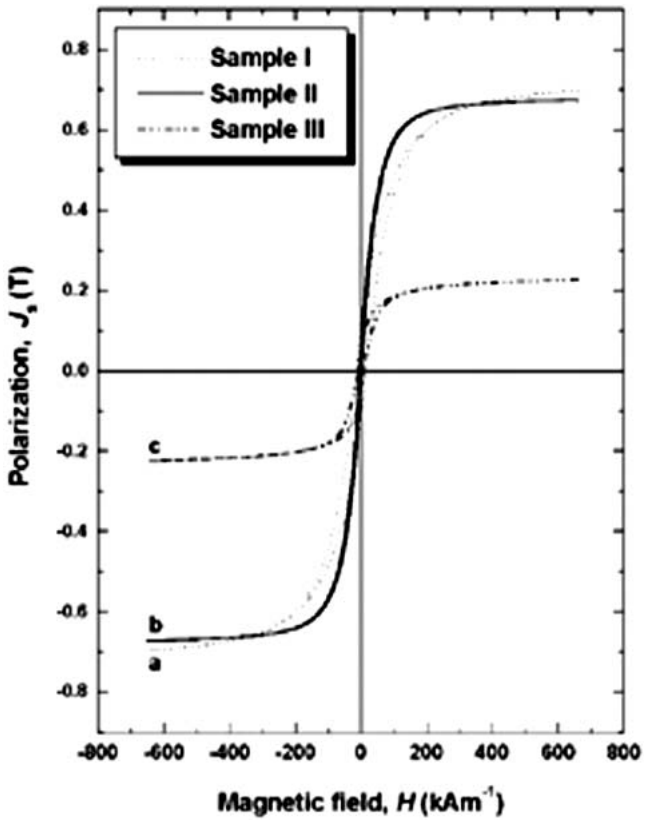

FIG. 10. Hysteresis *B–H* loops of previously mechanically alloyed $Co_{75}Ti_{25}$ powders for 11 ks and then heated to (a) 473 K, (b) 710 K, and (c) 993 K (see Fig. 6).

The enthalpy change of glass formation via TEGFR (ΔH_{TEGFR}) and enthalpy change of crystallization (ΔH_x) are presented in Fig. 14 as a function of the MA time. ΔH_{TEGFR} values were directly measured from the area under the low-temperature exothermic reaction during DSC measurements of the powders at the early stage of milling (see Fig. 6). ΔH_{TEGFR} monotonically decreases during the first few kiloseconds at the early stage of milling and approaches a minimum value of −0.56 kJ/mol after 11 ks of MA time. It, however, tends to disappear upon further MA time and completely vanished after 22 ks of MA time (Fig. 14). During the early stage of MA (0 to 11 ks) the ΔH_x does not change with changing MA time, and its values vary from −1.23 to −1.37 kJ/mol. It however, drastically decreased to −1.886 to −2.187 kJ/mol upon further ball-milling time (11 to 43 ks), indicating an increase in the volume fraction of the formed glassy phase.

IV. DISCUSSION

In contrast to the Co–Zr binary system, with its several deep eutectic compositions[31] which allow a wide glass-forming ability [see for example Ref. 32), the formation

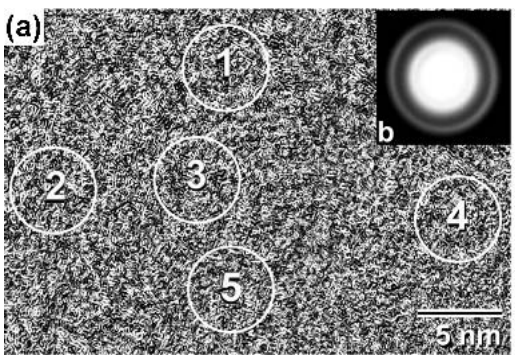

Region	Composition (at. %)	
	Co	Ti
1	76.8	23.2
2	73.4	26.6
3	76.2	23.8
4	74.1	25.9
5	72.7	27.3
av.	74.6	25.4

FIG. 11. (a) HRTEM and (b) the correlated SADP of previously mechanically alloyed $Co_{75}Ti_{25}$ powders for 11 ks and then heated to 710 K. The corresponding EDS analyses are listed in a table inside the figure.

of a glassy phase in the Co–Ti binary system has never, so far as we know, been reported in this system. This can be understood by looking at the phase diagram of this system, which does not show any deep eutectic compositions.[28] The first try for preparing an ordinary amorphous phase of $Co_{78}Ti_{22}$ alloy was demonstrated by Inoue *et al.*[28] when they reported the possibility of formation of an amorphous phase in a very narrow range (between 21 and 23 at.% Ti), using a melt-spinning method. This study confirms that a solid-state amorphization reaction takes place upon high-energy ball-milling of $Co_{75}Ti_{25}$ elemental powders under an argon gas atmosphere at room temperature. Either TEGFR or MIGFR processes, using the ball-milling technique, synthesized glassy $Co_{75}Ti_{25}$ powders. When the elemental $Co_{75}Ti_{25}$ powders are mechanically alloyed for a short MA time (1.8 to 3.6 ks), almost all the initial Co and Ti powders are agglomerated to form large composite particles, which contain large grains of the reactant materials [see Fig. 2(a)]. Further milling time (3.6 to 11 ks) leads to disintegrate these agglomerated powders and refine their "lamella" so that the number of layers/individual particle and their interfaces are monotonically increased. Such continuous intensive impact and shear forces that are generated by the milling tools (balls) create clean well-developed multilayered Co/Ti composite particles typical of sputtered or evaporated diffusion couples.[33–35] During the DSC experiments of these multilayered powders, two clear separate exothermic peaks appear (Fig. 6). The first exothermic reaction that appears at 661 K takes place due to a solid-state reaction between the thin elemental layers of Co and Ti [Fig. 8(a)], and this leads to the formation of a homogeneous [Figs. 8(e) and 8(f)] glassy phase [Figs. 9(b) and 11] with a composition closed to the starting nominal composition (see the EDS

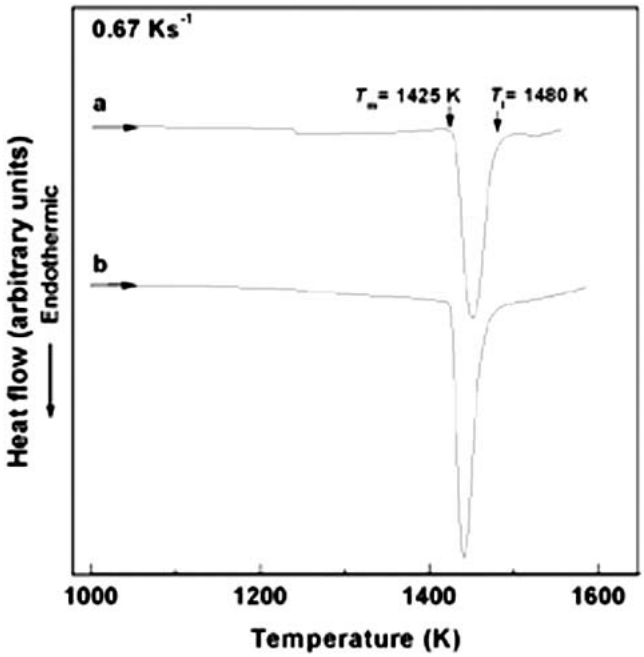

FIG. 12. DTA curves of (a) as mechanically alloyed $Co_{75}Ti_{25}$ powders for 11 ks and then heated to 710 K and (b) as mechanically alloyed $Co_{75}Ti_{25}$ powders for 86 ks. T_m is the melting temperature, whereas T_l is the liquidus temperature.

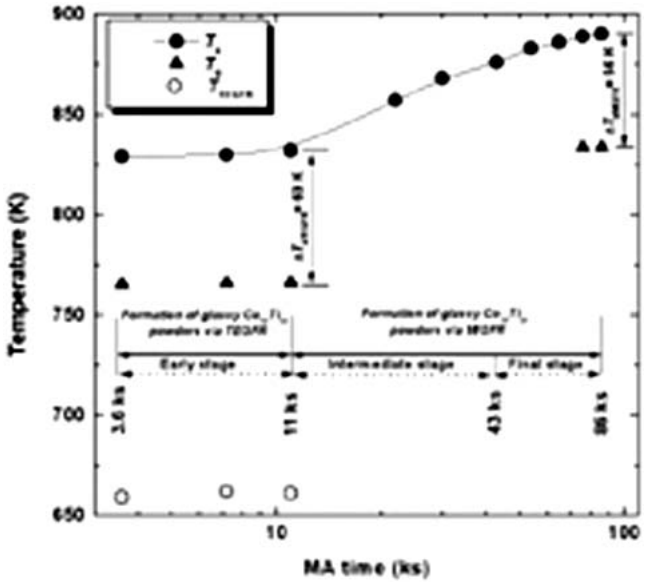

FIG. 13. Dependence of the T_{TEGFR} (○), T_g (▲), and T_x (●) on the MA time during ball-milling a mixture of $Co_{75}Ti_{25}$ powders. ΔT_{xTEGFR} and ΔT_{xMIGFR} refer to the supercooled liquid region ($\Delta T_x = T_x - T_g$) of the glassy phase that is formed by way of TEGFR and MIGFR processes, respectively.

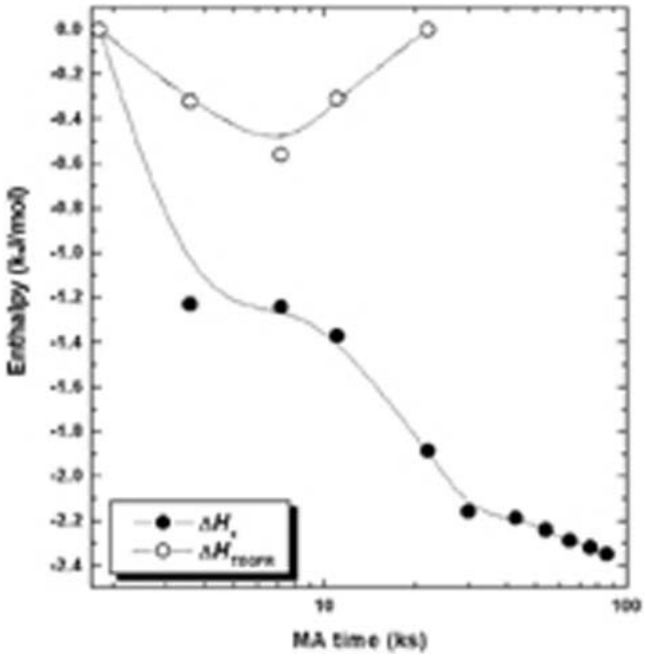

FIG. 14. Dependence of ΔT_{TEGFR} (○) and ΔH_{TEGFR} (●) on the MA time during ball-milling a mixture of $Co_{75}Ti_{25}$ powders.

analytical results in Fig. 11). The formation of a glassy phase via postannealing mechanically alloyed powders is not unique for the Co–Ti binary system. It has been recently shown by El-Eskandarany and Inoue[36] that a glassy phase of $Cu_{33}Zr_{67}$ alloy powders can be also obtained by isothermal annealing the multilayered composite powders at the early and intermediate stages of milling. Such a phenomenon was also reported for some mechanically alloyed metallic powders (see for example Refs. 15, 17, and 22). Indeed, postannealing the composite powder particles enhances the solid-state diffusion between the diffusion couples and this leads to a speeding up the rate of diffusion at the clean Co/Ti boundaries. Thus, the free energy changes drastically from a nonstable (the starting reactant materials) to a more stable phase (glass). For a successful TEGFR, the applied annealing temperature must be well below the temperatures that suppress the nucleation and growth of the equilibrium phase, i.e., crystallization temperature. The remarkable decrease in the polarization of as-annealed powders [Fig. 9(b)] suggests the completion of the solid-state reaction and the decrease of Co-free atoms in the composite powders upon annealing at 710 K.

In the MIGFR process, the solid-state reaction takes place in the same manner as occurs in the TEGFR process, except with a lower diffusion rate and a longer MA time [Figs. 1(c) and 1(d)]. This is attributed to the milling temperature that is assumed to be far below than in TEGFR (710 K). In the initial milling stage, crystalline elemental powders are mechanically crushed and fresh surfaces are highly created. Kneading of such ground powders enhances the atomic diffusion of elemental atoms and step-by-step local alloying.[23] Thus, the interdiffusion between Co and Ti layers occurs slowly. Because MA introduces many vacancies, lattice defects, grain boundaries, and surfaces, the ball-milled powders store a large amount of mechanical-strain energy.[37,38] Increasing the MA time during the intermediate stage of milling leads to continuous movements of the milling media which lead to an excess of the lattice imperfections that assist the diffusion between the Co–Ti diffusion couple, which have already a negative heat of mixing (−30 kJ/mol[39]). In the milling process, friction between balls and balls and the lining surface of a vial generates frictional heat. As a result of the balls' motion and their collisions, the interdiffusion in the multilayered powders is enhanced. In fact, such heat not only accelerates diffusion of constitutional atoms of the powder mixture but also contributes to thermal annealing of the unprocessed multilayered composite powders, which may remain in the mixture.

In contrast to the crystallization process of melt-spun $Co_{78}Ti_{22}$ taking place through two steps,[29] the as-mechanically alloyed $Co_{75}Ti_{25}$ transforms into the equilibrium phase of fcc-Co_3Ti through a single sharp exothermic reaction [Fig. 7(d)]. This is attributed to the high capability of the mechanically-induced solid-state reaction to homogenize the powders at the atomic scale during the different stages and to overcome the precipitation of any short- or medium-range order in the glassy matrix. The formed glassy phase at the last stage of milling is homogeneous, indicated by the near values of B_s, T_g, T_x, and ΔH_x of the powders (Figs. 5, 13, and 14). In addition, the EDS analyses for the final product of the glassy powders have not shown any significant concentration gradients or compositional fluctuations, indicating that the obtained glassy phases are uniform and homogeneous at the atomic scale.

V. CONCLUSIONS

High-energy ball-milling has been employed for fabrication of a single phase of glassy $Co_{75}Ti_{25}$ alloy powders at room temperature. During the early and intermediate stages of milling, postannealing of the mechanically deformed Co/Ti multilayered composite powders at 710 K leads to the formation of a glassy phase (TEGFR). The heat of glassy phase formation was directly measured and found to be −0.56 kJ/mol. When the elemental mixed powders are milled for a longer MA time (22 to 86 ks), the glass formation reaction is taking place due to mechanically-induced solid-state reaction. The final product, which is obtained after ball-milling for 86 ks, exhibits soft magnetic properties with polarization and coercivity values of 0.67 T and 2.98 kA/m, respectively. In addition, the glass transition temperature (T_g) takes place at a rather high temperature (833 K). This glassy alloy exhibits an extraordinarily high value of supercooled liquid region before crystallization, ΔT_x (56 K). The glassy powders obtained after 86 ks of MA time, crystallize through a single sharp exothermic reaction to the equilibrium phase of fcc-Co_3Ti upon heating to 889 K. The enthalpy change of crystallization (ΔH_x) and the reduced glass transition temperature (T_g/T_l) are −2.35 kJ/mol and 0.56, respectively.

REFERENCES

1. C.C. Koch, O.B. Cavin, C.G. McKamey, and J.O. Scarbrough, Appl. Phys. Lett. **43,** 1017 (1983).
2. M. Sherif El-Eskandarany, K. Aoki, and K. Suzuki, J. Less-Common Met. **167,** 113 (1990).
3. M. Sherif El-Eskandarany, K. Sumiyama, K. Aoki, and K. Suzuki, J. Mater. Res. **7,** 888 (1992).
4. M. Sherif El-Eskandarany, K. Sumiyama, and K. Suzuki, J. Mater. Res. **10,** 659 (1995).
5. M. Sherif El-Eskandarany, *Mechanical Alloying for Fabrication of Advanced Engineering Materials,* 1st ed. (William Andrew Publishing, New York, 2001), pp. 142–173.
6. A. Inoue, K. Matsuki, and T. Masumoto, Mater. Trans., JIM **31,** 148 (1990).

7. M. Sherif El-Eskandarany and A. Inoue, Metall. Mater. Trans. A. **33A,** 135 (2002).
8. M. Sherif El-Eskandarany and A. Inoue, J. Non-Cryst. Solids (2002, in press).
9. M. Sherif El-Eskandarany and A. Inoue, Metall. Mater. Trans. A. **33A,** 2145 (2002).
10. A. Inoue, in *Bulk Amorphous Alloys: Practical Characteristics and Applications,* edited by M. Magini and F.H. Wöhlbier (Trans Tech Publications, Vetikon-Zuerich, Switzerland, 1999), pp. 140–141.
11. J. Gottschall, Mater. Trans., JIM **42,** 548 (2001).
12. A. Inoue, in *Amorphous and Nanocrystalline Materials; Preparation, Properties and Applications,* 1st ed., edited by A. Inoue and K. Hashimoto (Springer Publishing, Berlin, Germany, 2001), pp. 47–48.
13. C. Fan and A. Inoue, Mater. Trans., JIM **38,** 1040 (1997).
14. R.B. Schwarz and C.C. Koch, Appl. Phys. Lett. **49,** 146 (1986).
15. R.B. Schwarz and R.R. Petrich, J. Less-Common Met. **140,** 171 (1988).
16. M. Sherif El-Eskandarany, K. Aoki, and K. Suzuki, Appl. Phys. Lett. **60,** 1562 (1992).
17. M. Sherif El-Eskandarany, K. Aoki, and K. Suzuki, J. Appl. Phys. **71,** 2924 (1992).
18. M. Sherif El-Eskandarany, K. Aoki, and K. Suzuki, J. Appl. Phys. **72,** 2665 (1992).
19. M. Sherif El-Eskandarany, Metall. Mater. Trans. **27A,** 3267 (1996).
20. M. Sherif El-Eskandarany, K. Aoki, K. Sumiyama, and K. Suzuki, Appl. Phys. Lett. **70,** 1679 (1997).
21. M. Sherif El-Eskandarany, K. Sumiyama, and K. Suzuki, Acta Mater. **45,** 1175 (1997).
22. M. Sherif El-Eskandarany, J. Alloys Compd. **284,** 295 (1999).
23. M. Sherif El-Eskandarany, K. Aoki, K. Sumiyama, and K. Suzuki, Acta Mater. **50,** 1113 (2002).
24. T. Mizushima, A. Makino, and A. Inoue, J. Appl. Phys. **83,** 6329 (1998).
25. A. Inoue, T. Zhang, T. Itoi, and A. Takeuchi, Mater. Trans., JIM **38,** 359 (1997).
26. B. Shen, H. Kimura, A. Inoue, and T. Mizushima, Mater. Trans., JIM **42,** 660 (2001).
27. H. Koshiba and A. Inoue, Mater. Trans., JIM **42,** 2572 (2001).
28. *Binary Alloy Phase Diagrams,* 2nd ed., edited by T.B. Massalski (ASM International, Materials Park, OH, 1992), Vol. 2, p. 1251.
29. A. Inoue, K. Kobayashi, C. Suryanarayana, and T. Masumoto, Scr. Metall. **14,** 119 (1980).
30. JADE card No. 23-0938.
31. *Binary Alloy Phase Diagrams,* 2nd ed., edited by T.B. Massalaki (ASM International, Materials Park, OH, 1992), Vol. 2, p. 1265.
32. K.H.J. Buschow, J. Less-Common Met. **85,** 221 (1982).
33. R.B. Schwarz and W.L. Johnson, Phys. Rev. Lett. **51,** 415 (1983).
34. B.M. Clements, W.L. Johnson, and R.B. Schwarz, J. Non-Cryst. Solids **61/62,** 817 (1984).
35. E.J. Cotts, W.J. Meng, and W.L. Johnson, Phys. Rev. Lett. **57,** 2295 (1986).
36. M. Sherif El-Eskandarany and A. Inoue, Mater. Trans., JIM **43,** 770 (2002).
37. A.E. Ermakov, E.E. Yurchikov, and V.A. Barinov, Phys. Met. Metall. **52,** 50 (1981).
38. A.W. Weeber, H. Bakker, and F.R. Boer, Europhys. Lett. **2,** 445 (1986).
39. F.R. de Boer, R. Boom, W.C.M. Mattens, A. Miedema, and A.K. Niessen, *Cohesion in Metals-Transition Metal Alloys* (North-Holland, Amsterdam, The Netherlands, 1988), p. 266.